Silicon (2019) 11:2853–2871
https://doi.org/10.1007/s12633-019-0072-9

ORIGINAL PAPER

Tribological Behaviour of Al6061–2SiC-xGr Hybrid Metal Matrix Nanocomposites Fabricated through Ultrasonically Assisted Stir Casting Technique

A. Prasad Reddy[1] · P. Vamsi Krishna[1] · R. N. Rao[1]

Received: 28 September 2018 / Accepted: 7 January 2019 / Published online: 2 February 2019

Abstract
This study deals with the tribological properties of 2 wt.% of SiC and x wt.% of Gr (x = 0, 0.5, 1, 1.5, 2, and 3) nanoparticles reinforced Al6061 alloy fabricated through ultrasonically assisted casting technique. Microstructure, various elements, particle sizes, phases, worn surfaces, wear debris are analyzed to understand the tribological behaviour of hybrid nanocomposites. Microstructural studies revealed the uniform dispersion of SiC and Gr nano-reinforcements in the matrix. Nano-clusters appeared in the micrographs with the increase of Gr nanoparticles. Density and microhardness of Al6061–2SiC-xGr hybrid nanocomposites decreased with the rise of Gr in the composite material. Influence of Gr content on the wear rate and coefficient of friction of hybrid nanocomposites are studied. Pin-on-disc apparatus is used to carry out the experiments at 5–20 N normal load, 0.5–2 m/s sliding velocity and 1000–3000 m sliding distance. The wear rate and coefficient of friction of hybrid nanocomposites reduced with the rise of nano Gr content up to a critical value and then increased. The reduction of wear rate for Al6061–2SiC-xGr (x = 0.5, 1, 1.5, 2, and 3) hybrid nanocomposites compared to AA6061 alloy at higher tribological conditions is 20%, 40.2%, 47.3%, 57%, 73%, and 64% respectively. Similarly the reduction in coefficient of friction for Al6061–2SiC-xGr (x = 0.5, 1, 1.5, 2, and 3) hybrid nanocomposites compared to Al6061 alloy is 3%, 5.9%, 11.8%, 17.7% and 9% respectively. The wear debris size decreased with the rise of Gr content in the Al6061–2SiC nanocomposite.

Keywords Hybrid metal matrix nanocomposites · Silicon carbide (SiC) · Graphite (Gr) · Wear rate · Wear debris

1 Introduction

In recent trends, the ceramic particles reinforced aluminium based composites have been used in various fields such as aerospace, structural, automobile and defense applications [1–3]. The demand is increasing day by day due to their good corrosion resistance, higher specific strength and better tribological properties [2]. It has been identified that the sliding characteristics of materials are of notable importance in tribological systems. It is noticed that the hard particles reinforced aluminum-based composites executed good strength and better tribological properties than the unreinforced aluminium and its alloys [3]. The strength and tribological properties of composites are dependent on various parameters such as reinforcement particle size (micro or nano), reinforcement content, reinforcement phase in the base material and type of fabrication process [4]. To improve the wear resistance of aluminium based composites researchers were added various ceramic reinforcement particles such as alumina (Al_2O_3), boron nitride (BN), silicon nitride (Si_3N_4), titanium dioxide (TiO_2), boron carbide (B_4C), molybdenum disulfide (MoS_2), silicon carbide (SiC), tungsten carbide (WC), tungsten trioxide (WO_3), titanium carbide (TiC) and titanium diboride (TiB_2) in the aluminum matrix [5–9]. Among them, SiC reinforcement particles have proven to be good compatibility with the aluminium alloys. The SiC reinforced aluminium nanocomposites resulted in improved wear resistance [10, 11]. SiC reinforced aluminium composites hold the promise for future growth due to their tailored properties, low cost, good forming characteristics and mass production capability [12–14]. Particularly in automobile sector, the SiC reinforced

✉ A. Prasad Reddy
aprasadreddy43@gmail.com

[1] Department of Mechanical Engineering, NIT Warangal, Telangana 506004, India

aluminium composite elements have been used like pistons, cylinder liners, connecting rod, gears, valves, pulleys, propeller shaft, engine cradle, bearing surfaces, camshafts, brake components, truck bodies and engine blocks [15–19]. In this wide variety of applications, the mechanical and tribological properties are very important. For better properties researchers have introduced various fabrication methods for hard nanoparticles reinforced aluminium nanocomposites. The fabrication techniques such as stir casting, squeeze casting, mechanical alloying and followed by hot compaction, powder metallurgy route, spark plasma sintering, laser deposition, spray deposition, and friction stir processing were investigated [5, 20–23]. Uniform dispersion of hard nano-reinforcement particles in the molten aluminium matrix is costly and lengthy process. Dispersion of nano-reinforcement particles through liquid metallurgical casting techniques i.e., compo casting and stir casting is complicated [20] due to the high surface area to volume ratio of the nanoparticles and poor wettability with the matrix [5].

Later many modifications have been done by the researchers in various liquid state metallurgical methods and introduced the ultrasonic-assisted stir casting method for better wettability and dispersion of hard nanoparticles in the aluminium alloy matrix [24–27]. In this method, nanoparticle clusters disintegrate into individual particles due to the variation in pressure gradient with high local temperatures [28–30]. During the ultrasonic process, molten metal purifies and grain refinement occurs [31]. Qiang et al. [32] fabricated Al/SiC nanocomposites through ultrasonic assisted stir casting technique and observed that the grain size of Al-SiC nanocomposites reduced with the addition of SiC nanoparticles. Yong et al. [33] fabricated A356/SiC nanocomposites through the ultrasonic-assisted casting method. The results revealed that SiC nano-reinforcement particles (2 wt.%) were well dispersed by reducing the formation of SiC nanoparticle clusters in the A356 alloy matrix by strong cavitation and acoustic streaming effects in molten metal. Srivastava et al. [28] produced Al6061-y (50 nm) Al_2O_3 (y = 1, 2, and 3 wt.%) nanocomposites by ultrasonic assisted stir casting process. The application of ultrasonic intensity resulted in better dispersion of Al_2O_3 nanoparticles in the matrix up to 2 wt.%. The addition of Al_2O_3 nanoparticles above 2 wt.% led to poor distribution, clusters of Al_2O_3 nanoparticles and microcracks were induced in the Al6061 alloy matrix. Prasad et al. [34] fabricated Al6061-SiC (50 nm) nanocomposites through ultrasonic assisted stir casting technique. The addition of SiC nanoparticles above 2 wt.% led to the formation of more nanoparticle clusters and poor distribution in the matrix. The viscosity of the molten melt increases with the rise of SiC nanoparticle content in the matrix and which reduces the efficiency of ultrasonic treatment. Therefore, the reduction in efficiency of ultrasonic treatment would be resulting in more nanoparticle clustering [28]. The Al6061-SiC nanocomposites exhibited better tribological properties at 2 wt.% of SiC nano-reinforcement particles. Several investigations have proven that the ceramic nanoparticles were distributed uniformly in the alloy matrix through the ultrasonic- assisted casting process. Better dispersion of hard nanoparticles in the molten metal would be depending on the various process parameters such as processing time, processing temperature, ultrasonic pressure, weight percent of nanoparticles and ultrasonic intensity [35].

The wear rate of sensitive parts such as cylinder heads, liners, pistons and drive shafts in the automobile assembly unit has been improved by reinforcing SiC particles in the aluminum matrix [36]. Zou et al. [37] noticed that the wear rate of SiC particles reinforced Al-Si-Cu based composites was lower than that of Al-Si-Cu matrix. The depth of penetration into the subsurface and plastic flow of pin material on surface decreased by reinforcing SiC particles in the base material. Researchers [38] examined the wear properties of Al5252/SiC composites with varying reinforcement particle size. Tribological properties of Al5252-SiC nanocomposites are good compared to the micron-sized SiC particles reinforced Al5252/SiC composites. Micron size particles reinforced Al5252/SiC composites has higher wear resistance when applied normal loads are minimal. The nanoparticles reinforced Al5252/SiC composites revealed superior wear resistance at higher applied normal loads. Mazahery and Shabani [39] studied the tribological properties of Al6061/SiC composites with varying average reinforcement particle size and its content. The hardness of material and applied normal load on pin have significant influence on tribological properties during dry sliding of Al6061/SiC composites. Manivannan et al. [10] examined the tribological properties of Al6061/SiC nanocomposites. The reports revealed that the wear rate of nanocomposite is lower than the Al6061 alloy. Shirazi et al. [11] reported the wear properties of Al6061/SiC nanocomposites. The study revealed that the rise of SiC content in the Al6061 alloy material improved the hardness and reduces the wear loss. Better mechanical and tribological properties were observed for SiC nanoparticles reinforced aluminum based nanocomposites due to the presence of primary phase SiC nanoparticles and rise of dislocations in the base material [2]. The SiC nanoparticles act as barriers to the disloctions movement under applied external loads on the matrix. Many experiments were proved that the incorporation of SiC nano-reinforcement particles in the aluminium based alloy increases the friction between the contact surfaces [40]. Reason for damage of automobile and machine parts are due to the heavy friction and wear. An appropriate solid lubricant is added for reducing the coefficient of friction and improving the wear behaviour of the SiC reinforced aluminium based composite materials during dry sliding [41].

Researchers were conducted experiments to examine the wear properties of aluminium based composites by

introducing SiC as primary reinforcement and a solid lubricant as secondary reinforcement in the matrix material at various tribo parameters [42, 43]. Addition of solid lubricant as secondary reinforcement in the matrix is for better wear properties and reduction in coefficient of friction of the Al/SiC nanocomposites. Carvalho et al. [44] examined the wear behavior of AlSi-CNTs-SiC hybrid nanocomposites at dry condition on reciprocating pin-on-plate. The wear rate was reduced by reinforcing CNTs as primary reinforcements and SiC as secondary reinforcements in the Al-Si matrix. Babu et al. [45] noticed the minimal wear loss and friction coefficient for A356–10 vol.%Al_2O_3–10 vol.% GNF hybrid nanocomposites. Results show that an enhancement in wear resistance and reduction in friction coefficient for more than 15 vol.% of GNF (graphite nanofiber) and Al_2O_3 fiber reinforced composites. This could be due to the presence of GNFs and Al_4C_3 agglomerations within the matrix. The Gr particles are the most extensivley used solid lubricant in the aluminium based matrix due to its low cost and yield better tribological properties with SiC, Al_2O_3 and B_4C particles [14, 46]. Aruri et al. [45] described that the decrease in wear rate of Al6061-SiC-Al_2O_3 and Al6061-SiC-Gr hybrid composites. Reduction in wear rate is due to the incorporation of various ceramic reinforcements (i.e SiC, Al_2O_3 and Gr). SiC reinforcement particles bear the external applied load and Gr act as a solid lubricant in the Al6061-SiC-Gr hybrid nanocomposites. Liu et al. [47] examined tribological properties of Al2014-5vol. %Gr composite. The Gr reinforced Al2014 alloy based composite revealed minimum wear loss and friction coefficient than that of base material. Ames and Alpas [48] studied wear properties of A356–20%SiC-3%Gr hybrid composite. Results revealed that higher wear resistance with the introduction of SiC and Gr particles. Improvement in wear resistance was attributed to the load bearing effect of SiC reinforcement particles and its abrasive nature. Ravindran et al. [46] investigated the tribological properties of Al2024-5 wt.% SiCp-5 wt.% Gr hybrid composites. Hardness and wear resistance of hybrid composites improved due to the increase of SiC and Gr nano-reinforcement particles in the base material. Significant wear resistance was observed for Al2024-5 wt.% SiCp-5 wt.% Gr based hybrid nanocomposites. Mostafapour and Khandani [49] examined the Al5083-Gr-Al_2O_3 hybrid nanocomposites. The nanocomposite with Gr of 75% hybrid ratio resulted in reduced wear rate and friction coefficient. Suresha and Sridhara [50] prepared LM25 aluminium alloy-SiC-Gr hybrid composites. The wear rate of hybrid composites was reduced than LM25-SiC composites. Jaswinder et al. [51] specified that the friction coefficient reduced by reinforcing 6 wt.% Gr in Al/10 wt.% SiC composite. An increase in mechanical properties of Al/10SiC/6Gr hybrid composite is due to the addition of SiC and Gr reinforcements in the matrix. Basavarajappa et al. [52] produced Al2219/15SiC composite and Al2219/15SiC/3Gr hybrid composites. Gr reinforced hybrid composite revealed the lower degree of subsurface deformation than the non-Gr reinforced composite and the deformation was increased with rising the sliding velocities. Manivannan et al. [53] fabricated the Al6061-(0.4–1.6 wt.%) of SiC (50 nm)/(0.5 wt.%) of Gr (20 μm) Gr hybrid nanocomposites by ultrasonically assisted casting method. The reports specified that the wear rate and friction coefficient of the hybrid composites were lower than the Al6061 alloy at various applied normal loads. The incorporation of solid lubricant as secondary reinforcements in the Al-SiC hybrid nanocomposites improved the tribological properties. There is a scope for Al/SiC/Gr hybrid nanocomposites in various tribological systems such as automobile industry and aircraft applications including engine block, engine valves, pistons and cylinders due to their good sliding characteristics [16]. Utilization of Al/SiC/Gr hybrid nanocomposite elements in an automobile assembly unit led to reduce the usage of oil and service cost.

From the literature it is observed that the hybrid nanocomposites are better choice compared to nanocomposites. However, the secondary reinforcement used in previous studies are micro level or hybrid nanocomposites were fabricated by other than ultrasonic assisted process. Due to various applications and better properties of hybrid nanocomposites, in depth study of its tribological properties is necessary. In the present study, the Al6061–2 wt.% of SiC-x wt.% of Gr (x = 0, 0.5, 1, 1.5, 2 and 3) hybrid nanocomposites are manufactured through ultrasonically assisted stir casting technique. SiC (50 nm) and Gr (<1 μm) nanoparticles effect on tribological properties of Al6061/SiC/Gr hybrid composites was examinied. Tribological properties of these Al6061/2SiC/xGr hybrid nanocomposites is studied under different conditions. Scanning electron microscopy (SEM) and Energy dispersive X-ray spectroscopy (EDAX) were used to study the worn surfaces and wear debris. Possible wear mechanisms of Al6061–2SiC-Gr hybrid nanocomposites are discussed in detail.

2 Materials and Methods

Bharat Aerospace Metals, India supplied the commercial grade of Al6061 alloy in the T6 condition. The elemental composition of Al6061 alloy was magnesium (Mg-0.93), silicon (Si-0.52), iron (Fe-0.25), copper (Cu-0.18), manganese (Mn-0.14), zinc (Zn-0.09), chromium (Cr-0.07), nickel (Ni-0.03), titanium (Ti-0.01) and aluminium (Al-97.78). β-SiC nano-powder of average particle size 50 nm was procured from US Research Nanomaterials, Inc., USA. Graphite (Gr) particles of average particle size 500 nm were supplied by Mknano, M K Impex Corp., Canada. The SiC and Gr particles were analyzed under transmission electron microscopy (TEM) to ensure the size of the particles shown in Fig. 1.

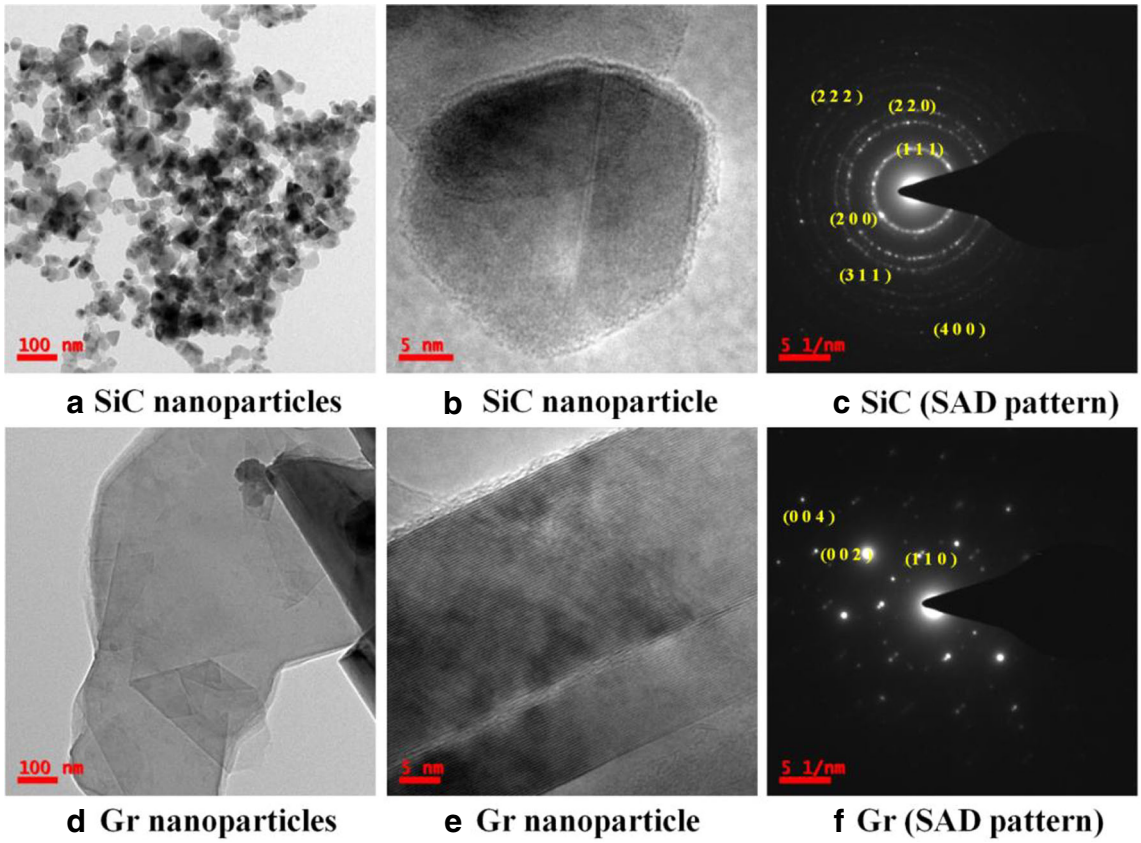

Fig. 1 TEM micrographs of SiC and Gr nanoparticles

The schematic view of ultrasonically assisted casting setup used for manufacturing of hybrid nanocomposites is shown in Fig. 2. The experimental setup consists of an electrical resistance heating furnace, thermocouples, ultrasonic unit, air compressor for cooling the ultrasonic generator, furnace control unit, and the argon supply unit. Ultrasonic horn of 20 mm diameter made up of Ti-10Al-4 V alloy coated with zirconia (ZrO_2) was used to transmit ultrasonic waves at 20 kHz frequency with maximum power 2.4 kW. A commercially pure Al6061 alloy ingot of 600 g was melted at 750 °C in a steel crucible of inner diameter 70 mm, outer diameter 78 mm and length 120 mm. Upon reaching 780 °C, nano-sized SiC and Gr particles enclosed with aluminium foil and preheated up to 550 °C and fed into the Al6061 alloy molten melt. The mechanical stirrer was used to mix the nano-sized SiC and Gr particles into the Al6061 alloy molten metal for about 10 min. The ultrasonic probe was preheated to 780 °C and inserted into the Al6061 alloy melt to a depth of about 25 mm for 5 min. The ultrasonic processed molten composition was poured into a mild steel mold, which was preheated to 550 °C. The Al6061 alloy, Al6061–2 wt.% SiC-x wt.% Gr (x = 0, 0.5, 1, 1.5, 2 and 3) hybrid nanocomposites were fabricated through ultrasonically assisted casting technique under protective argon atmosphere. The fabricated nanocomposites are named as 2NC (x = 0), 0.5HNC (x = 0.5), 1HNC (x = 1), 1.5HNC (x = 1.5), 2HNC (x = 2) and 3HNC (x = 3).

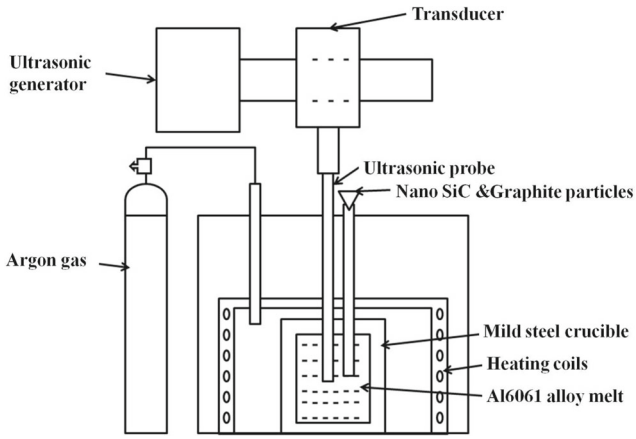

Fig. 2 Schematic setup of ultrasonically assisted stir casting

2.1 Material Characterization, Density and Hardness Measurement

The morphology of materials was characterized using SEM and EDS of TESCAN Make Model Vega LMU 3. Crystal

structure and phases of the base alloy, SiC, Gr, and nanocomposites were analyzed through XRD. The fabricated specimens were prepared for SEM studies using 200, 400, 600, 800, 1000, and 1200 grit papers respectively. After polishing, the specimens were etched with 25 ml methanol (CH_2O), 25 ml hydrochloric acid (HCl), 25 ml nitric acid (HNO_3) and one drop of hydrofluoric acid (HF) for 40 s. The composite pin specimens and wear debris were analyzed under SEM after dry sliding wear test. Density of Al6061 alloy (2.7 g/cm^3) [28], SiC (3.218 g/cm^3) [10] and Gr (2.266 g/cm^3) [54] was observed from the literature. The theoretical, experimental density and microhardness [55] measurement methods was discussed in reference [34]. The average microhardness value was noted from six readings.

2.2 Wear Rate Measurement

Wear tests were conducted as per G 99–05 ASTM standards using the pin-on-disc setup of Magnum Model-TE-165 [34, 56]. Wear test process parameters used in experiments is shown in Table 1. The pin samples were cleaned with acetone before performing the wear tests. After performing the wear test, wear rates were calculated from Eqs. 1 and 2. All the tests were repeated for three times and the average value was taken individually.

$$\Delta V_l = \frac{m_i - m_f}{\rho} \tag{1}$$

$$W_l = \frac{\Delta V_l}{SD} \tag{2}$$

Where, ΔV_l volume loss; $(m_i - m_f)$ change in mass; ρ density of pin specimen; SD is sliding distance of pin and W_l volume metric wear rate.

3 Results and Discussion

3.1 Microstructure and Phase Analysis of Materials

Figure 3 represents the SEM micrographs of Al6061 alloy, 2NC nanocomposite, 0.5HNC, 1HNC, 1.5HNC, 2HNC, and 3HNC hybrid nanocomposites. Figure 3a indicates the unreinforced Al6061 alloy. Figure 3b shows the microstructure of 2NC nanocomposite. The grayish white SiC nanoparticles are present in Al6061 alloy matrix and uniformly distributed in the matrix. However, few smaller SiC particle clusters are observed in the matrix. Figure 3c, d, e, f, and g depicts the microstructure of 0.5HNC, 1HNC, 1.5HNC, 2HNC, and 3HNC hybrid nanocomposites. It reveals that SiC and Gr nano-reinforcements are dispersed uniformly in the Al6061 alloy matrix. However, small-scale nano-clusters appeared in the microstructure with the rise of Gr quantity in the matrix.

XRD analysis of Al6061 alloy, SiC, Gr, 2NC nanocomposite, 0.5HNC, 1HNC, 1.5HNC, 2HNC, and 3HNC hybrid nanocomposites is presented in Fig. 4. The properties of the nanocomposites are influenced by the nature of the reinforcing material used. XRD studies have been used for identification of phases in the nanocomposites. The phases of nanocomposites are recognized through JCPDs software. In XRD pattern peaks(2θ) have been observed in the ranging from 20° to 90°. XRD spectrum confirms the presence of strong diffraction peaks at 2θ values of 38.43° for (111), 44.56° for (020), 64.94° for (022), 78.3° for (311), and 82.14° for (222) planes belongs to aluminium (JCPDS Card No.89–4037). The strong diffraction peaks at 2θ values of 35.68° for (111), 41.44° for (200), 60.1° for (220), 71.8° for (311) planes belongs to SiC (JCPDS Card No. 74–2307). The strong diffraction peaks at 2θ values of 35.68° for (111), 44.38° for (101), 54.57° for (004), 72.71° for (110) planes belongs to C (JCPDS Card No. 75–1621).

Table 1 Tribological test process parameters used in experiments

Tribological parameters (Units)	Experimental Conditions
Applied normal load (N)	5, 10, 15, 20
Sliding speed (m/s)	0.5, 1, 1.5, 2
Sliding distance (m)	1000, 2000, 3000
Materials	Al6061 alloy, 2NC, 0.5HNC, 1HNC, 1.5HNC, 2HNC, 3HNC
Temperature (°C)	25 ± 2
Humidity (%)	67 ± 2
Surface roughness, Ra (μm)	0.21
Repeated test for each sample	3
Pin diameter (mm)	8
Pin length (mm)	25
EN31 steel disc diameter (mm)	165
EN31 steel disc thickness (mm)	8

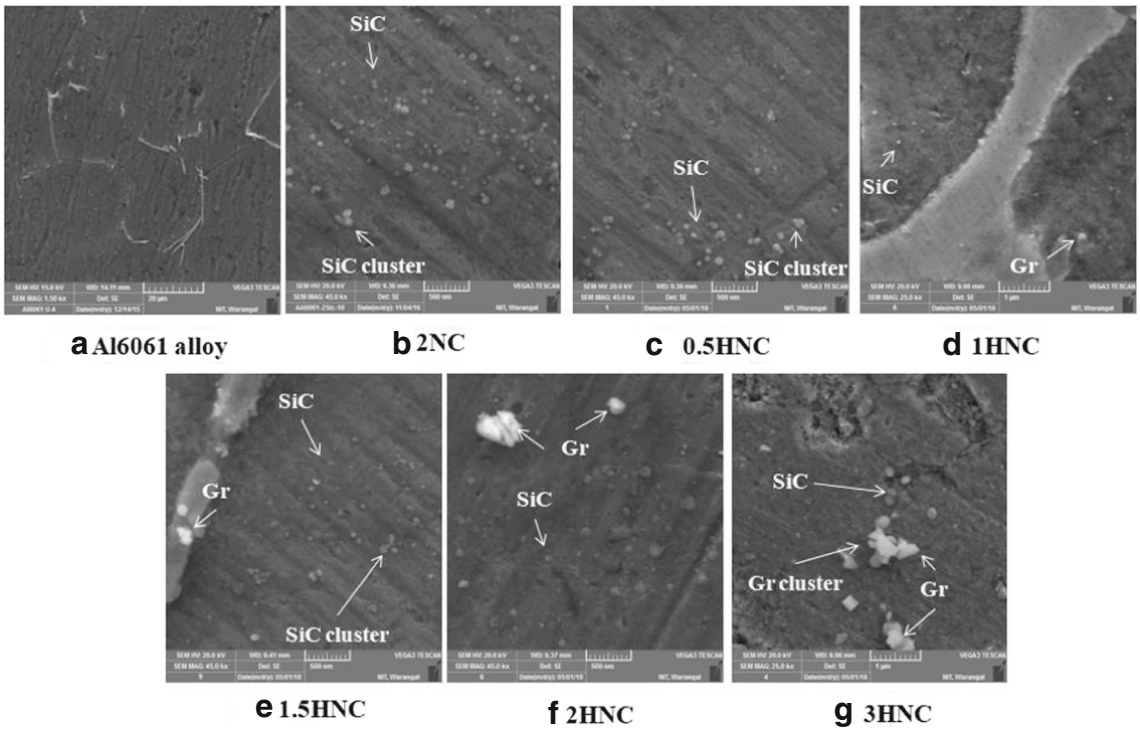

Fig. 3 SEM micrographs of Al6061 alloy based materials

The intensity of peak is lower for C and SiC due to lower content in the matrix. The intensity of peaks of C doesn't appear in the 0.5HNC and 1HNC hybrid nanocomposite due to its lower content in the matrix.

3.2 Density and Hardness of Pin Materials

The theoretical density, experimental density, porosity and microhardness of the Al6061 alloy, 2NC nanocomposite,

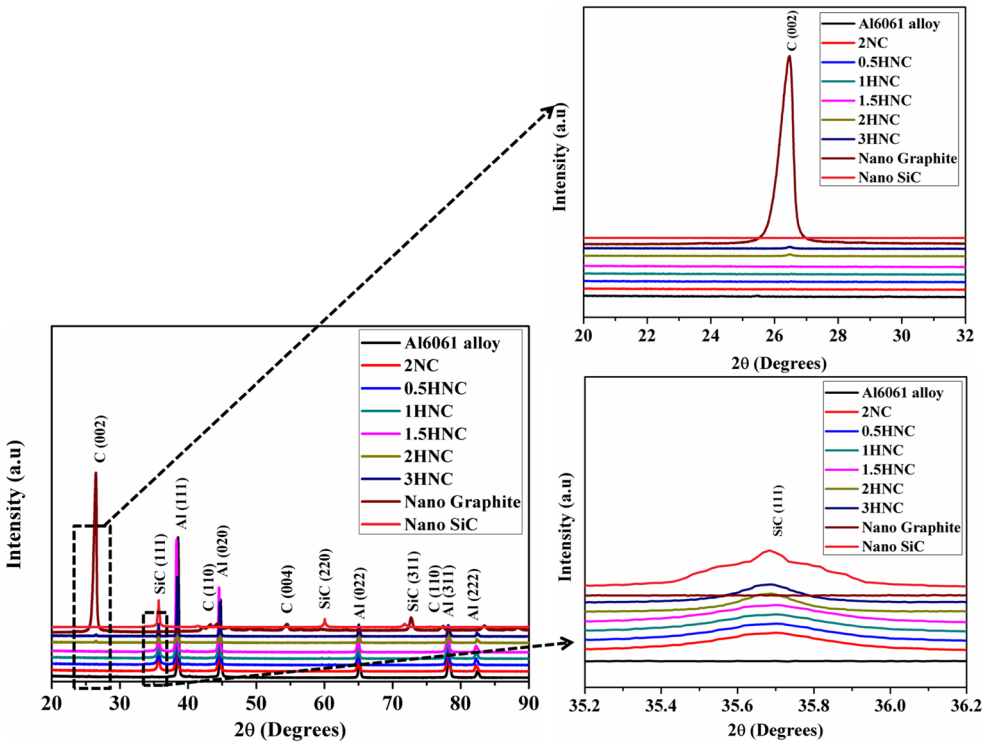

Fig. 4 XRD of pure Al6061 alloy, 2NC, 0.5HNC, 1HNC, 1.5HNC, 2HNC, and 3HNC hybrid nanocomposites

Table 2 Density and microhardness of various materials

Properties/Materials	Theoretical density (g/cm^3)	Experimental density (g/cm^3)	Porosity (%)	Microhardness (HV)
Al6061 alloy	2.7	2.685	0.56	52 ± 3
2NC	2.74	2.709	1.13	91 ± 4
0.5HNC	2.71	2.669	1.51	89 ± 2
1HNC	2.704	2.648	2.1	87 ± 2
1.5HNC	2.701	2.603	2.5	85 ± 2
2HNC	2.698	2.594	2.9	83 ± 2
3HNC	2.695	2.569	3.2	76 ± 3

0.5HNC, 1HNC, 1.5HNC, 2HNC, and 3HNC hybrid nanocomposites represented in Table 2.

It is noticed that the density of hybrid nanocomposites reduced due to the presence of a lower density of Gr powder compared to the nanocomposite and base material. Density of 0.5HNC, 1HNC, 1.5HNC, 2HNC, and 3HNC hybrid nanocomposites is decreased by 1%, 1.4%, 3.1%, 3.4%, and 4.3% respectively. Porosity of Al6061–2SiC-xGr hybrid nanocomposites increased with the increase of wt. % Gr in the matrix. This would be attributed to the rise in contact surface area of Gr nanoparticles with air and more quantity of air occupy some space in the molten metal during ultrasonic operation. Similarly the rise in porosity of nanocomposites reported with increase of weight percent in the matrix [57]. Microhardness of hybrid nanocomposites increased compared to base alloy and decreased compared to nanocomposite. The reduction in microhardness of the Al6061–2SiC-xGr hybrid nanocomposites could be due to the presence of Gr. The Gr being soft allotrope of carbon and acts as a solid lubricant. The Gr will ease the grain movement along slip planes due to its weak van der Waals forces of parallel thin plates.

3.3 Wear Rate of Pin Materials

Wear rate of Al6061 alloy, 2NC nanocomposite, 0.5HNC, 1HNC, 1.5HNC, 2HNC, and 3HNC hybrid nanocomposites is presented in Fig. 5. Figure 5a, b represent the wear rate of materials with respect to applied normal load at 0.5 m/s, 1000 m (named as V_LD_L) and 2 m/s, 3000 m (named as V_HD_H) conditions respectively. Figure 5c, d indicate the wear rate of hybrid nanocomposites as a function of sliding velocity at 5 N, 1000 m (named as L_LD_L) and 20 N, 3000 m (named as L_HD_H) conditions respectively. Figure 5e, f depict the wear rate of hybrid nanocomposites as a function of sliding distance at 0.5 m/s, 5 N (named as V_LL_L) and 2 m/s, 20 N (named as V_HL_H) conditions respectively. The test conditions 5 N, 1000 m and 0.5 m/s; 5 N, 3000 m and 2 m/s; 20 N, 1000 m and 0.5 m/s; 20 N, 3000 m and 2 m/s are named as $L_LD_LV_L$, $L_LD_HV_H$, $L_HD_LV_L$ and $L_HD_HV_H$ respectively. It is identified that the wear rate of all materials increased gradually with the rise of applied normal loads [40]. The higher wear rate is found in unreinforced Al6061 alloy compared to composite materials. This would be attributed due to less wear resistance of unreinforced Al6061 alloy at all applied normal load conditions. During dry sliding, counteracting of hard asperities would lead to the formation of large grooves with a higher depth of penetration and larger deformation of surface leads to more wear rate [58]. It is identified that the wear rate of materials rises with the increase of sliding velocity and sliding distance. Temperature at the interaface of the composite pin and EN31 steel disc increases with rise of sliding velocity and which induces the oxidation phenomenon. Heavy heat dissipation at the interfaces of the pin and EN31 steel counterface reflects on chemical structure of the pin material [59]. The rise of temperature at the interface would be resulting in higher wear rate of material due to the worn-off of lubricating film [60]. In many studies, researchers have been reported that the tribo-layer worn off with the increase of contact surface temperature and thus results in higher wear rate [61]. It is identified highest wear rate for unreinforced Al6061 alloy as compared to 2NC nanocomposite and hybrid nanocomposites at all conditions.

It is observed that 2NC nanocomposite revealed good wear resistance than base material. This would be due to the formation of mechanically mixed layer (MML) of soft Al6061 alloy matrix and hard ceramic nano-sized SiC particles. SiC nanoparticles mixed with MML and reduce the transfer of material from the pin surface and hence improves the wear resistance [62]. The SiC nanoparticles act as a barrier to the external applied load and increase the hardness of nanocomposite. Due to the higher hardness and smaller size, as the detached SiC nanoparticles rolled between the surfaces and played a part in a three-body abrasion mechanism by contributing towards abrading the two mating surfaces [63, 64]. These hard asperities of EN31 steel chips and SiC nanoparticles penetrate furthermore into the matrix with the rise of loads and sliding velocity. The rise in temperature introduces the oxide layer formation with the mixer of SiC nanoparticles at $L_HD_HV_H$ conditions. At the interface, harder asperities penetrate into the pin surface and

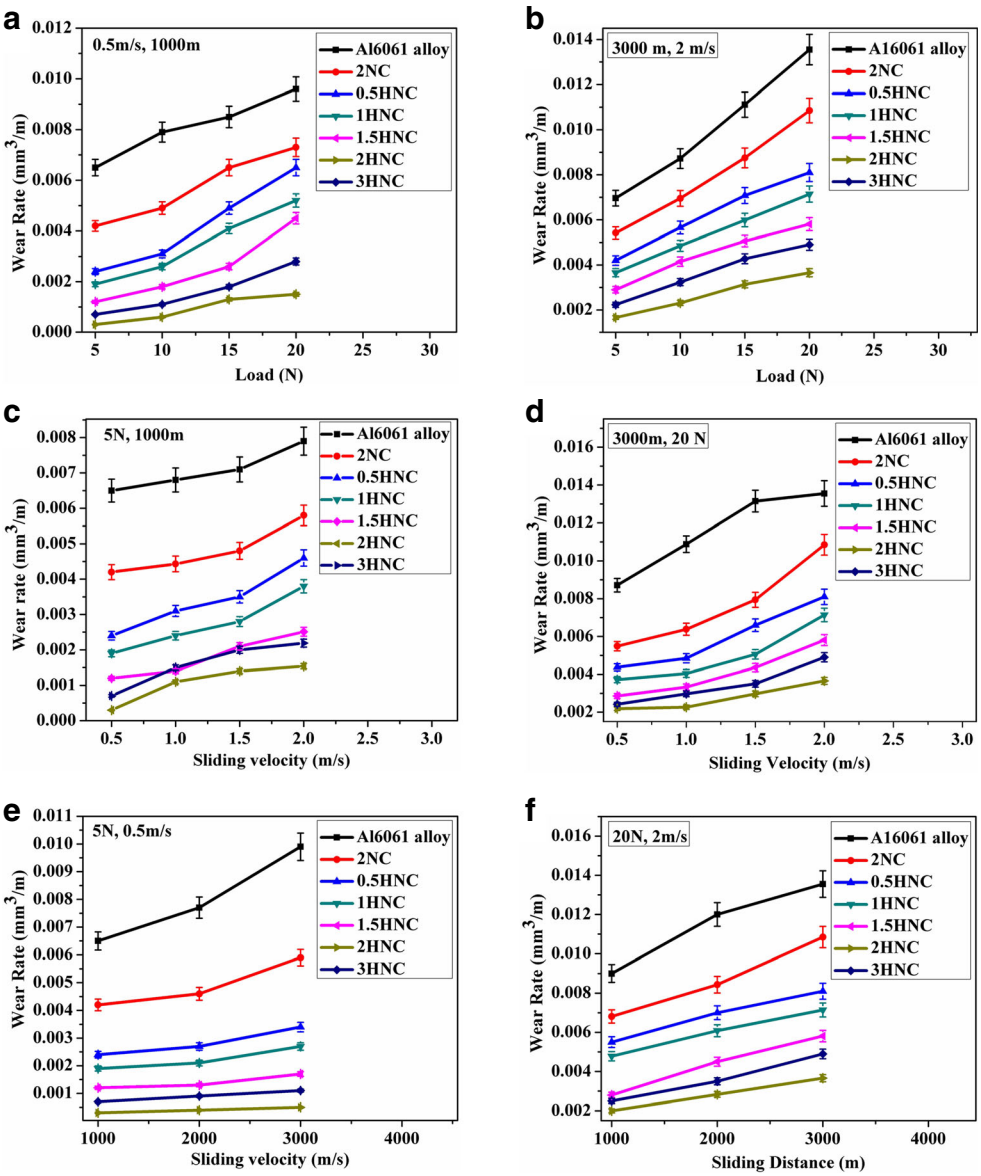

Fig. 5 Wear rate (WR) of Al6061 alloy based composite materials (**a**) WR verses load at V_LD_L, (**b**) WR verses load at V_HD_H, (**c**) WR verses sliding velocity at L_LD_L, (**d**) WR verses sliding velocity at L_HD_H, (**e**) WR verses sliding distance at V_LL_L, and (**f**) WR verses sliding distance at V_HL_H

damage the oxide layer at higher load and sliding velocity and hence increase in the wear rate [65, 66]. As can be seen that from the Fig. 5e, f, the sliding distance doesn't affected much on the wear rate as compared to the effect of load and sliding velocity. Favourable effect of SiC nanoparticles in improving the wear resistance has also been reported by other researchers [11, 67].

It is noticed from Fig.5, the wear rate of 0.5HNC, 1HNC, 1.5HNC, 2HNC, and 3HNC hybrid nanocomposites reduced with increasing the Gr content in the base material and raised with increasing the applied normal loads and sliding velocity. This would be attributed due to the continuous supply of Gr, the formation of Gr thick film and spreading over the contact surface of the pin without peeling off. Incorporation of Gr as a secondary phase in the soft matrix result in the formation of a more stable lubricating layer on the tribo-surface of hybrid nanocomposites compared to the base alloy and nanocomposite [8]. Reduction in wear rate of the hybrid nanocomposites with rise of Gr content would be related to the dual phase effect of SiC and Gr nanoparticles in the formation of stronger MML on the contact surface. The aluminium based hybrid composites consisting of dual phases of SiC and Gr particles in the matrix possess better tribological properties than the Al-SiC based composites and alloy. In another report specified that rise in sliding velocity as a function of load is expected rise in surface temperature and more severe wear [68]. It can be seen that from Fig. 6 that the wear rate of all hybrid nanocomposites has lower wear rate than alloy and nanocomposite. The reduction in wear rate for 2NC nanocomposite, 0.5HNC, 1HNC, 1.5HNC, 2HNC, and 3HNC hybrid nanocomposites

compared to Al6061 alloy at $L_HD_HV_H$ is 20%, 40.2%, 47.3%, 57%, 73%, and 64% respectively. The sudden reduction is observed in wear rate for 3HNC hybrid nanocomposite. This would be attributed to the formation of a thick lubricating Gr layer on the tribo-surface, porosity, and cracks [69]. The thick lubricating Gr layer peels off from the pin surface at V_HL_H conditions.

3.4 Coefficient of Friction of Pin Materials

The average friction coefficient values of Al6061 alloy, 2NC nanocomposite, 0.5HNC, 1HNC, 1.5HNC, 2HNC, and 3HNC hybrid nanocomposites is presented in Fig. 7. It is identified that from Fig. 7a, b the average coefficient of friction increased with increasing loads on pin irrespective of materials. Reports revealed that the friction coefficient increased by incorporation of SiC nanoparticles in the base material. It would be attributed to the appearance of cubic structured beta-SiC nanoparticles in the base material [70]. However, the friction coefficient reduced with rise of Gr nanoparticle content in the 2NC nanocomposite at a particular applied normal load. The average friction coefficient values of the hybrid nanocomposites is lower than the 2NC nanocomposite and base alloy. The hard SiC nanoparticles withstand the load and Gr nanoparticles acted as a solid lubricant and reduce the pin-counterface contact area and resulted in reduction of the friction coefficient values [71]. Increase of friction coefficient values would be attributed due to the rise of the depth of penetration with an increase of tangential loads on the pin. However, at higher applied normal load conditions, the strong interface bond between SiC, Gr nanoparticles, and the matrix tend to breaks down and the average coefficient of friction values increases significantly. Figure 7c, d represent the friction coefficient values with respect to sliding velocity. Results reveal that the average friction coefficient values redues slightly with rise of sliding velocity for all materials.

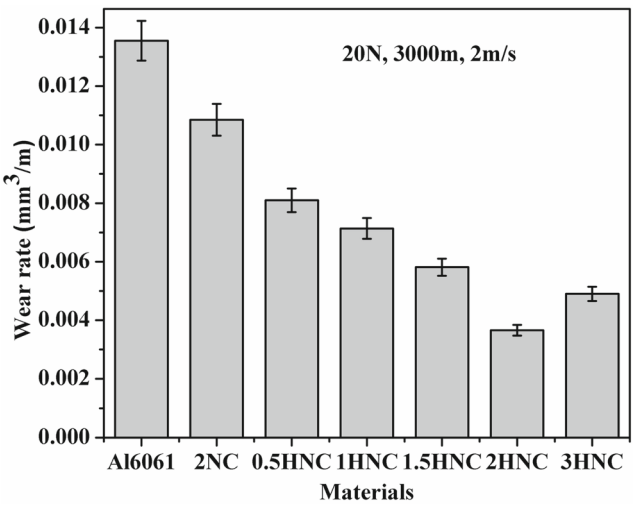

Fig. 6 Wear rate of Al6061 alloy based materials at $L_HD_HV_H$ condition

It is identified that the friction coefficient values is lower at higher sliding velocity. It would be attributed to the softening of both the composite pin specimen and the EN 31 steel disc during dry sliding. At higher sliding velocity, the frictional heat is higher resulting in a higher flash temperature at the contact points [72]. Incorporation of Gr nanoparticles minimizes the heat generation due to friction by its lubricity. Further reduction in the friction coefficient values in the case of hybrid nanocomposites at higher sliding velocities would be due to the introduction of Gr tribo-layer on the contact surface.

Figure7e, f depict the friction coefficient values with respect to sliding distance. The variation of friction coefficient values is very high throughout the beginning stages of sliding and decrease with sliding distance, as seen in Fig. 8. The friction coefficient values reduce slightly with the increase of sliding distance. The decrease in the friction coefficient values is related to the type of wear mechanism [54]. Interactions of hard asperities at the interface would influence the friction coefficient values during dry sliding period [60]. This would be due to the formation of the mixer of SiC and Gr nanoparticles with the MML layer and which reduces the friction coefficient. Decrease of friction coefficient of hybrid nanocomposite is due to the hexagonal structure of graphite and which act as a solid lubricant [69]. The exhibited results shown in Fig. 8 reveals that the lower friction coefficient for 2HNC hybrid nanocomposite compared to all materials. The reduction of the coefficient of friction of 0.5HNC, 1HNC, 1.5HNC, 2HNC, and 3HNC hybrid nanocomposites compared to Al6061 alloy at $L_HD_HV_H$ is 3%, 5.9%, 11.8%, 17.7%, and 9% respectively. The experimental results also confirm the increase of coefficient of friction for 3HNC hybrid nanocomposite with more than 2 wt% of Gr addition. After reaching the critical value of Gr addition increases the formation of thick Gr tribo-layer on the worn surface would be pealing-off from the surface and causes the higher depth of penetration of asperities on the counter surface and leads to larger resistance to its sliding movement. The wear resistance of the aluminium based materials increased by the addition of Gr reinforcement particles more than the critical value resulted in increasing the coefficient of friction [73].

3.5 Worn Surfaces of Pin Samples

Figures 9, 10, 11 and 12 represent the worn surfaces of Al6061 alloy, 2NC nanocomposite, 0.5HNC, 1HNC, 1.5HNC, 2HNC and 3HNC hybrid nanocomposites at $L_LD_LV_L$, $L_LD_HV_H$, $L_HD_LV_L$ and $L_HD_HV_H$ conditions. In Figs. 9a and 10a indicate the worn surfaces of Al6061 alloy at 5 N applied load, lower and higher sliding distance, and sliding velocity conditions respectively. It can be observed that parallel grooves, scratches, and plastic deformation at

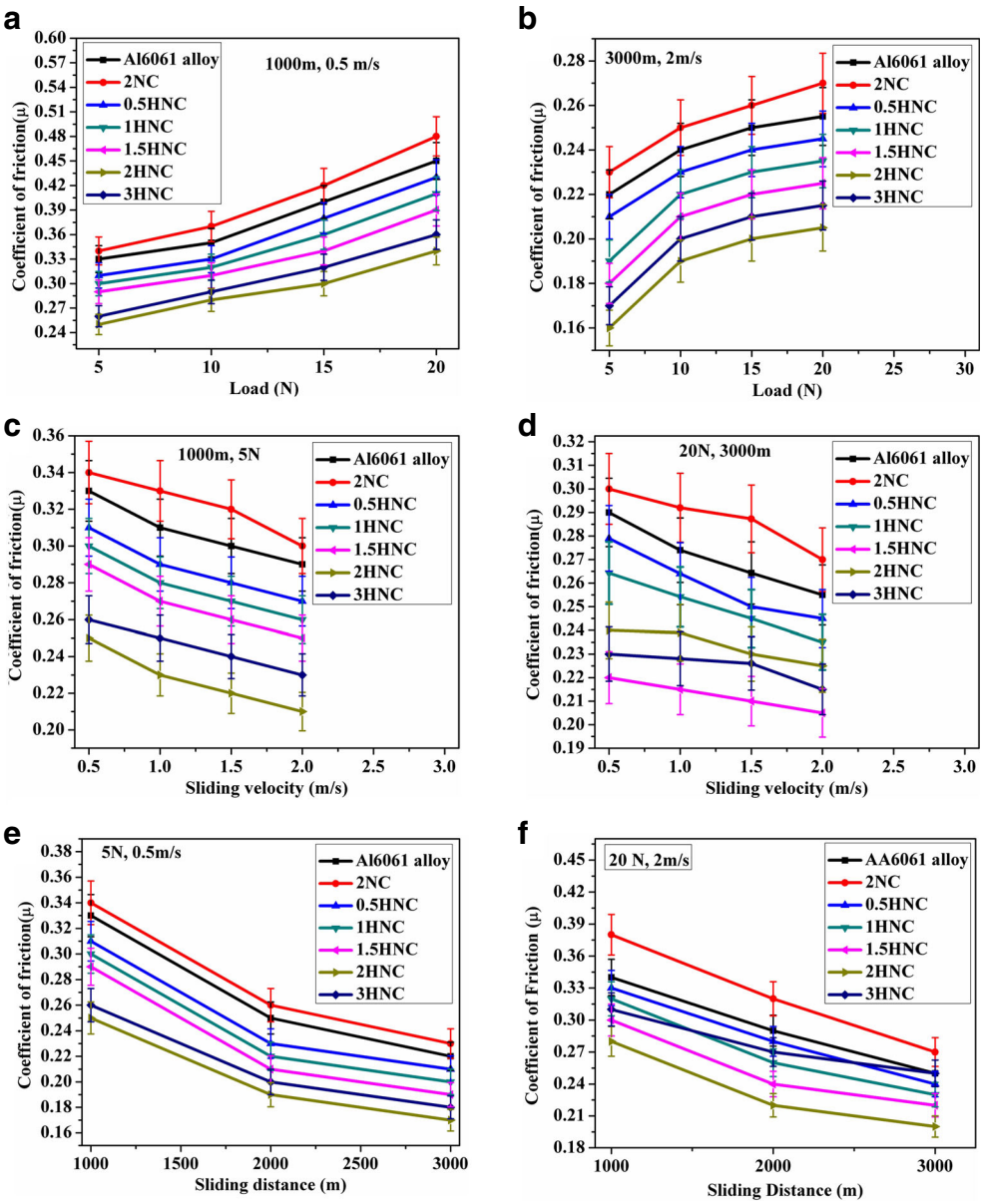

Fig. 7 Friction coefficient (FC) values of Al6061 alloy based composite materials (**a**) FC verses load at V_LD_L, (**b**) FC verses load at V_HD_H, (**c**) FC verses sliding velocity at L_LD_L, (**d**) FC verses sliding velocity at L_HD_H, (**e**) FC verses sliding distance at V_LL_L, and (**f**) FC verses sliding distance at V_HL_H

$L_LD_LV_L$ condition. Deep grooves, shallower scratches and plastic flow are observed at $L_LD_HV_H$ condition. In Figs. 11a and 12a depict the worn surfaces of Al6061 alloy at $L_HD_LV_L$ condition. It can be seen that deeper parallel grooves, scratches and higher plastic flow at $L_HD_LV_L$ condition. Deep grooves, shallower scratches and turbulent flow of material is observed at $L_LD_HV_H$ condition. The execution of grooves and scratches on pin surface would be the evidence of abrasive wear mechanism (denoted as A). The plastic flow occurred on the surface in the sliding direction with a row of furrows is an indication of adhesive wear mechanism (denoted as B). The increase of either load or sliding velocity increases the plastic deformation with the higher depth of penetration [74]. It is attributed to the lower hardness of unreinforced Al6061 alloy.

In Figs. 9b and 10b represent the worn surfaces of 2NC nanocomposite at $L_LD_LV_L$ condition. Formation of smaller scratches in the sliding direction is evident of abrasive wear mechanism (denoted as A). The SEM micrograph of the worn surface of 2NC nanocomposite reveals that the delamination mechanism (denoted as D) in the sliding direction. It reveals that the lower plastic deformation in the sliding direction and which is lower than the unreinforced Al6061 alloy at $L_LD_LV_L$ condition. It reveals that the delamination of material in the sliding direction at $L_LD_HV_H$ condition. In Figs. 11b and 12b represent the worn surfaces of 2NC nanocomposite at $L_HD_LV_L$ condition. The worn surface of 2NC nanocomposite reveals that the shallower scratches with higher plastic deformation at $L_HD_LV_L$ condition. The worn surface of 2NC nanocomposite reveals the turbulent plastic flow of

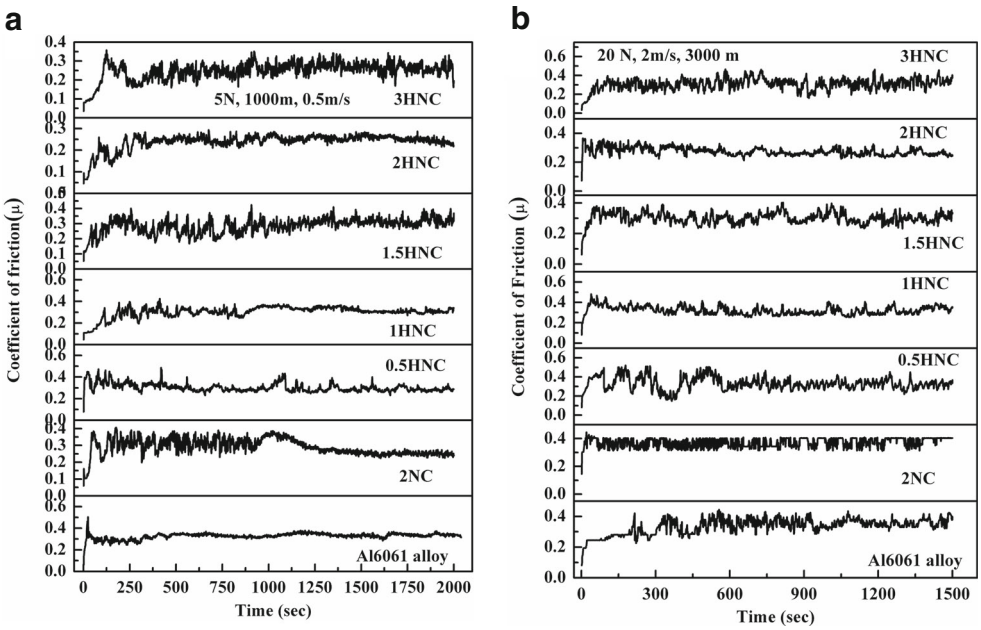

Fig. 8 Friction coefficient of Al6061 alloy based materials (**a**) $L_LD_LV_L$, and (**b**) $L_HD_HV_H$

material in the sliding direction at $L_HD_HV_H$ condition. The depth of penetration is less compared to the unreinforced alloy at all conditions. This would be attributed to the presence of nano-sized SiC reinforcement particles in the Al6061 alloy matrix and which hinder the plastic flow of material during dry sliding.

Figures 9c, d and e, 10c, d and e, 11c, d and e, 12c, d and e shows the worn surfaces of 0.5HNC, 1HNC and 1.5HNC hybrid nanocomposites at $L_LD_LV_L$, $L_LD_HV_H$, $L_HD_LV_L$ and $L_HD_HV_H$ conditions. It is identified that the Gr thin film (denoted as G) spread over the surface but not covered the entire surface. The worn surface of hybrid nanocomposites reveals that the lower plastic deformation at $L_LD_LV_L$ conditions. At this condition depth of penetration is lower than the unreinforced alloy and 2NC nanocomposite. It is observed that more depth of penetration, where the Gr thick layer is not present on the pin surface at $L_LD_HV_H$ condition. The uncovered surface reveals the higher plastic deformation and obtained wear mechanism is abrasive wear at $L_HD_LV_L$ condition. It is observed that the Gr thin film formed with gaps on

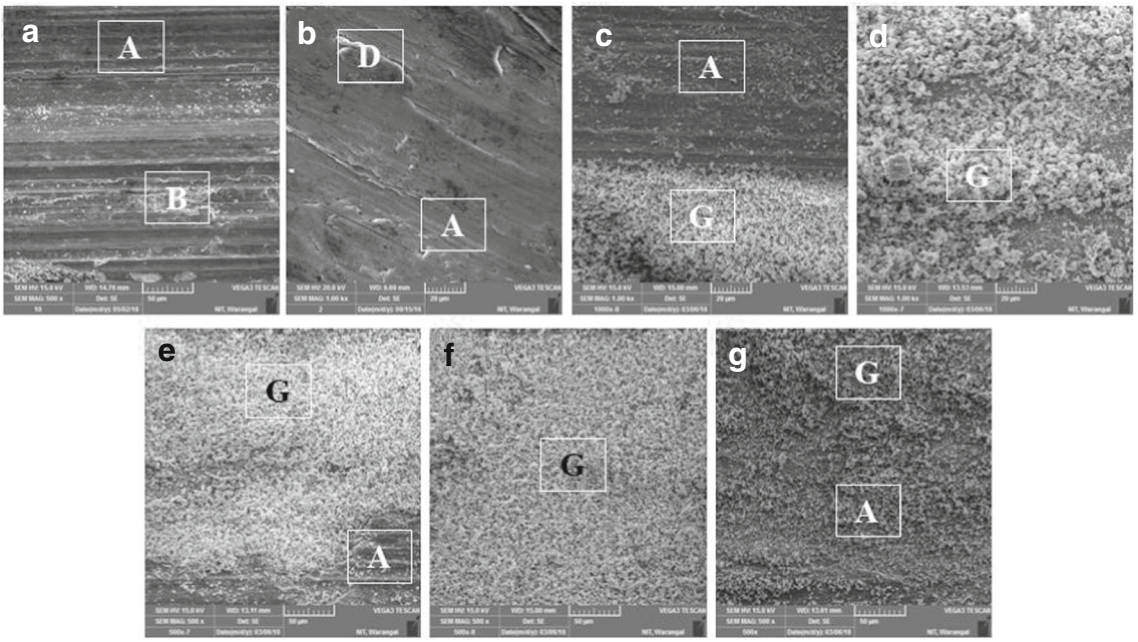

Fig. 9 SEM micrographs of worn surfaces at $L_LD_LV_L$ condition (**a**) Al606l alloy, (**b**) 2NC, (**c**) 0.5HNC, (**d**) 1HNC, (**e**) 1.5HNC, (**f**) 2HNC, and (**g**) 3HNC

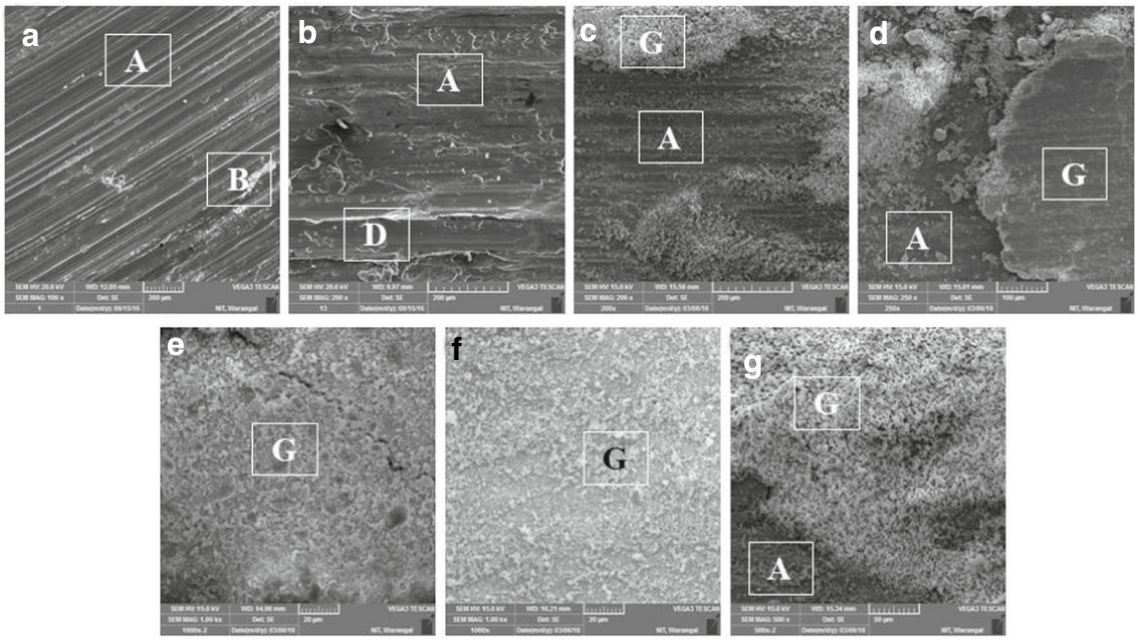

Fig. 10 SEM micrographs of worn surfaces at $L_LD_HV_H$ condition (**a**) Al6061 alloy, (**b**) 2NC, (**c**) 0.5HNC, (**d**) 1HNC, (**e**) 1.5HNC, (**f**) 2HNC, and (**g**) 3HNC

the worn surface at $L_HD_HV_H$ condition. This is due to lack of continuous supply of Gr thin film on the pin surface during dry sliding wear. The increase of Gr content in the matrix decreases the groove formation and depth of penetration. Available Gr content on the worn surface acts as a solid lubricant and which prevents the severe damage of the pin material. It is found that at low Gr content in the 2NC nanocomposite, the effect of Gr as a solid lubricant in dry sliding condition is very less.

Figures 9f, 10f, 11f and 12f show the worn surfaces of 2HNC hybrid nanocomposite at $L_LD_LV_L$, $L_LD_HV_H$, $L_HD_LV_L$ and $L_HD_HV_H$ conditions. On the worn surface of the hybrid nanocomposite, the thick Gr film is spread over the surface without gaps and cracks at all conditions. It is observed that the Gr thin film well distributed over the worn surface and executed the abrasive wear mechanism. During dry sliding the sheared Gr particles forms thick lubricating layer and reduce the direct contact of pin and steel counter

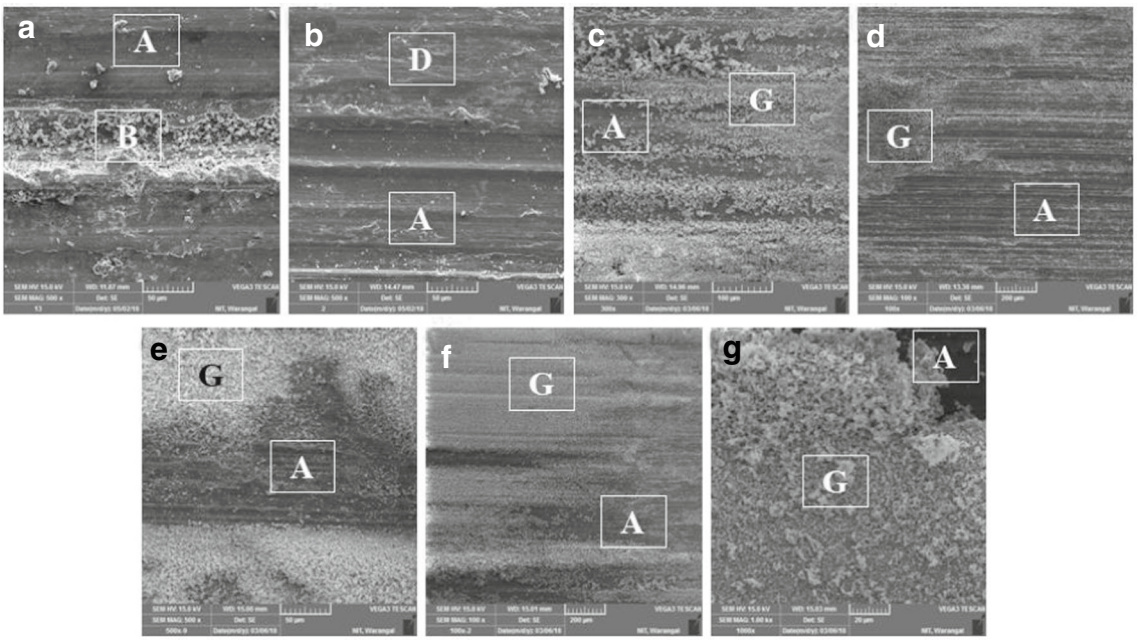

Fig. 11 SEM micrographs of worn surfaces at $L_HD_LV_L$ condition (**a**) Al 6061 alloy, (**b**) 2NC, (**c**) 0.5HNC, (**d**) 1HNC, (**e**) 1.5HNC, (**f**) 2HNC, and (**g**) 3HNC

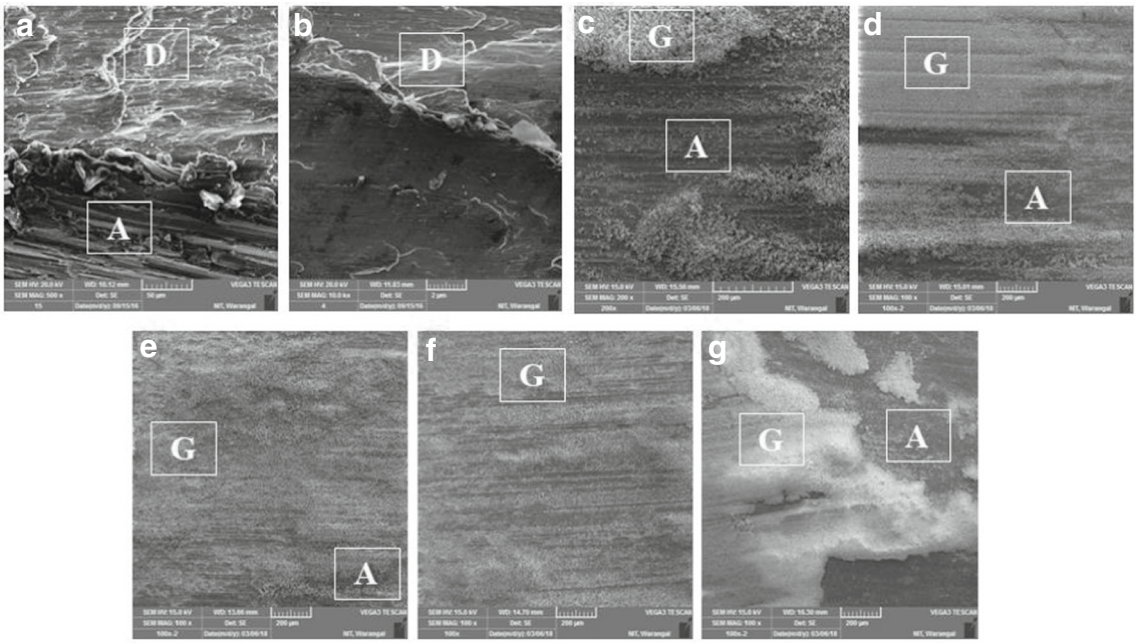

Fig. 12 SEM micrographs of worn surfaces at $L_HD_HV_H$ condition (**a**) Al6061 alloy, (**b**) 2NC, (**c**) 0.5HNC, (**d**) 1HNC, (**e**) 1.5HNC, (**f**) 2HNC, and (**g**) 3HNC

face. The depth of penetration is less compared to lower content Gr reinforced hybrid nanocomposites, unreinforced alloy and 2NC nanocomposite. Figures 9g, 10g, 11g and 12g shows the worn surfaces of 3HNC hybrid nanocomposite at $L_LD_LV_L$, $L_LD_HV_H$, $L_HD_LV_L$ and $L_HD_HV_H$ conditions. It is observed that the Gr layer sheared and spread over the worn surface during dry sliding at 5 N load conditions. At 20 N load conditions the micrographs reveal that the Gr thick film spread over the surface and peeling off Gr film in some area. It would be attributed to oversupply of Gr on the surface $L_HD_HV_H$ condition. Due to the peeling off Gr thick film from the surface, increases the depth of penetration and which is less compared to the unreinforced Al6061 alloy and 2NC nanocomposite. Due to the continuous supply of Gr reaches to the saturated state during dry sliding and the Gr thick film peeling off from the worn surface then executed the abrasive wear mechanism. The addition Gr content in the 2NC nanocomposite above the critical value, it is found that the due to the release of Gr to the worn surface during dry sliding Gr thick film forms and Gr film peeling off from the pin surface and increases the wear rate.

3.6 EDAX Analysis

Figures 13 and 14 represent the EDAX analysis of 2HNC hybrid nanocomposite at conditions $L_LD_LV_L$ and $L_HD_HV_H$ conditions. The elemental analysis of the worn surface reveals that the mixture of constituents from pin material, disc material and iron based oxide compounds. From the EDAX analysis it can be seen that the peaks of carbon (C), iron (Fe), aluminium (Al), silicon (Si), and oxygen (O).

The EDAX analysis of Gr thick layer covered area of worn surface of hybrid nanocomposite tested at 5 N load condition reveals that the low intensity of Al, Fe and O, high intensity of C peaks. The higher intensity C peak reveals that the presence of smeared nano Gr on pin worn surface. The presence of higher intensity of C peak minimizes the plastic deformation of Al6061 alloy matrix. The EDAX of Gr uncovered layer (named as spectrum 2) worn surface of hybrid nanocomposite reveals low intensity of C peak, higher intensity of Al, Fe, and O peaks at 5 N load condition. Worn surface of Gr thick layer covered hybrid nanocomposite tested at 20 N load condition reveals higher intensity of C, O, and Fe peaks and low intensity of Al peak. At similar conditions the uncovered (named as spectrum 2) Gr thick film area exhibited high intensity of Al peak and low intensity of Fe where as O peak at 20 N load condition. It indicates that the higher plastic deformation due to absence of Gr film on the worn surface.

3.7 Wear Debris of Pin Materials

Figure 15 represents the wear debris of Al6061 alloy, 2NC nanocomposite and 2HNC hybrid nanocomposite. In Fig. 15a indicates that the larger size wear debris produced from Al6061 alloy during dry sliding condition. Formation of large size wear debris would be attributed to the severe plastic

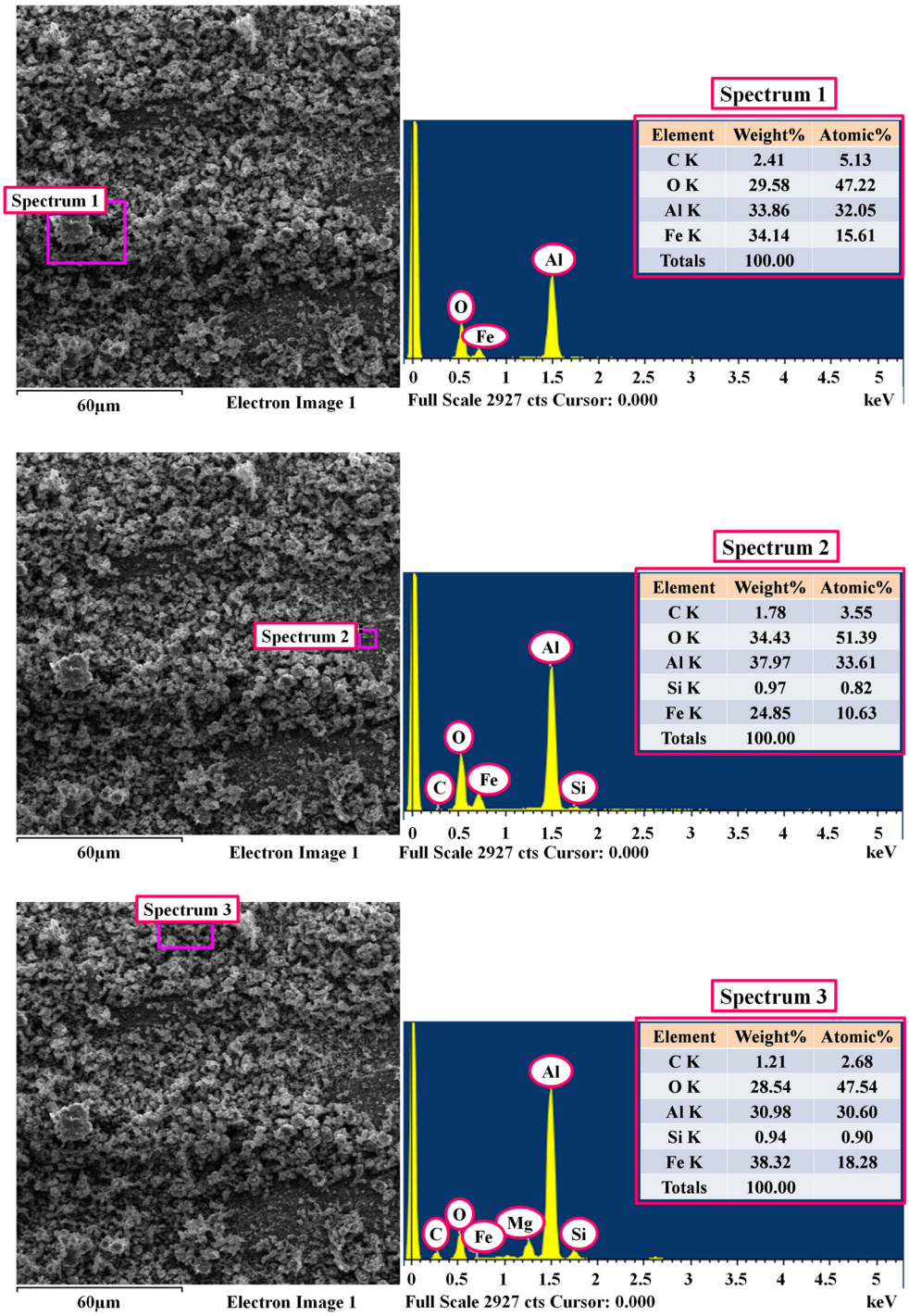

Fig. 13 EDAX analysis of 4HNC hybrid nanocomposite worn surface at $L_L D_L V_L$ condition

deformation with higher depth of penetration of hard asperities of steel disc counter face during dry sliding condition. From Fig. 15b represents the Al6061 alloy matrix is filled with SiC nano-reinforcements with lower inter particle spacing and which increases the dislocation density.

The medium size wear debris produced from 2NC nanocomposite. The production of medium size wear debris may be due to the application of external loads starts yielding of dislocation pile up in the subsurface of the pin material [75]. The contact profile of 2NC nanocomposite shows the yielding of dislocation piles up, which lead to crack initiation and propagates towards subsurface layer. The SiC nano-reinforcement particles come out from the subsurface and combined with the MML and increase the wear resistance. The SiC nano-reinforcement particles resist the hard asperities from the steel disc counter face and hence reduce the plastic deformation and higher depth of penetration. From Fig. 15c it is observed that the lower inter particle spacing for 2HNC

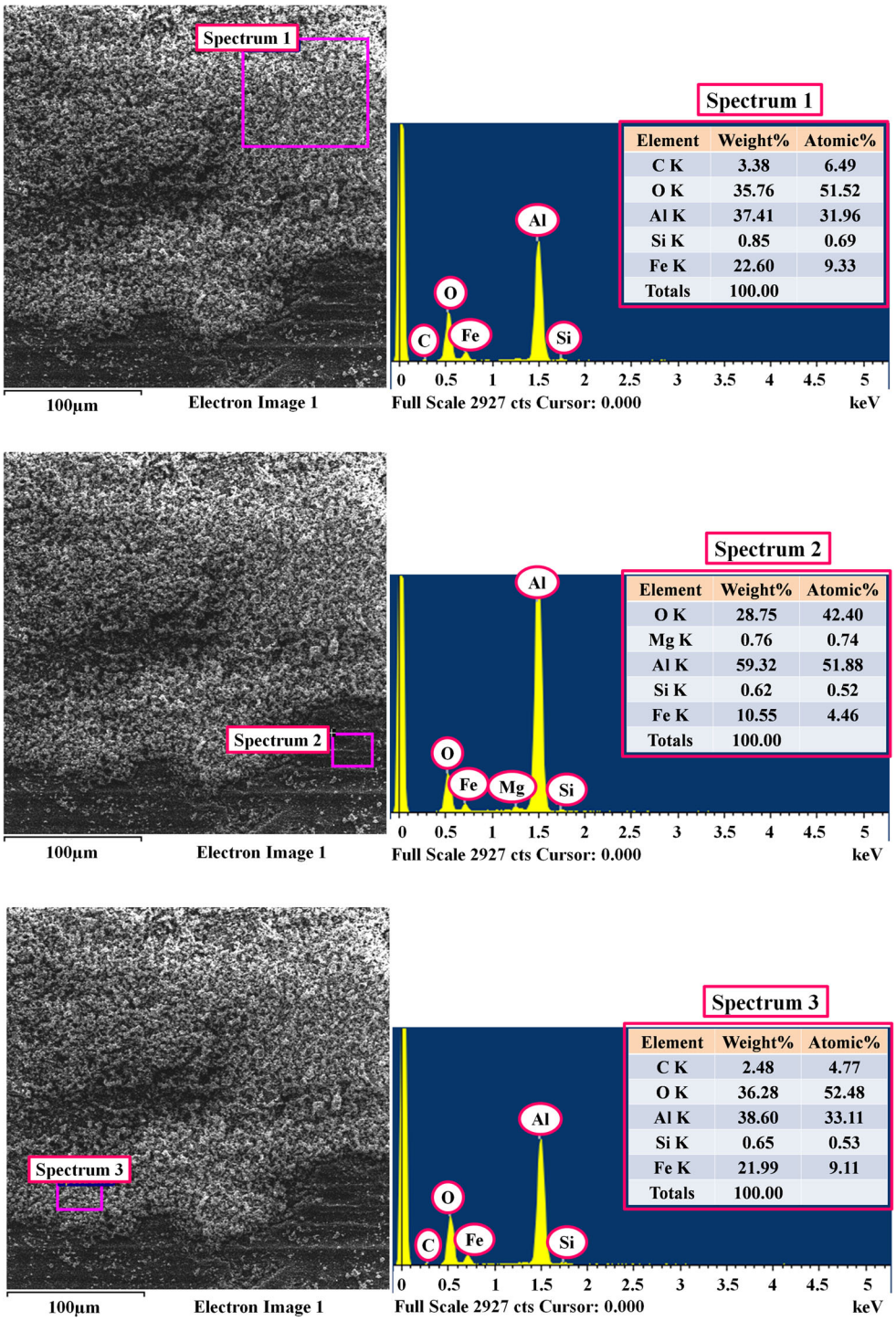

Fig. 14 EDAX analysis of 2HNC hybrid nanocomposite worn surface at $L_H D_H V_H$ condition

hybrid nanocomposite. It would be due to the rise of dislocations with the addition SiC and Gr nano-reinforcements in the matrix. It is seen that the lower depth of penetration and MML with SiC and Gr nano-reinforcements in the contact profile of 2HNC hybrid nanocomposite. It is observed that the finer size wear debris produced from 2HNC hybrid nanocomposite during dry sliding wear. The size reduction of wear debris of 2HNC hybrid nanocomposite would be due to the production of continuous thick Gr layer on the pin contact surface mixed with MML and SiC nano-reinforcements. The hard particle dislocation density increases in the thick Gr layer which leads to reduction of contact between the pin surface and steel disc counter face. Figure 16 shows the EDAX analysis of wear debris of 2HNC hybrid nanocomposite. It reveals that the existence of iron and oxygen in the wear debris. The appearance of iron in the wear debris implies the transfer of iron from

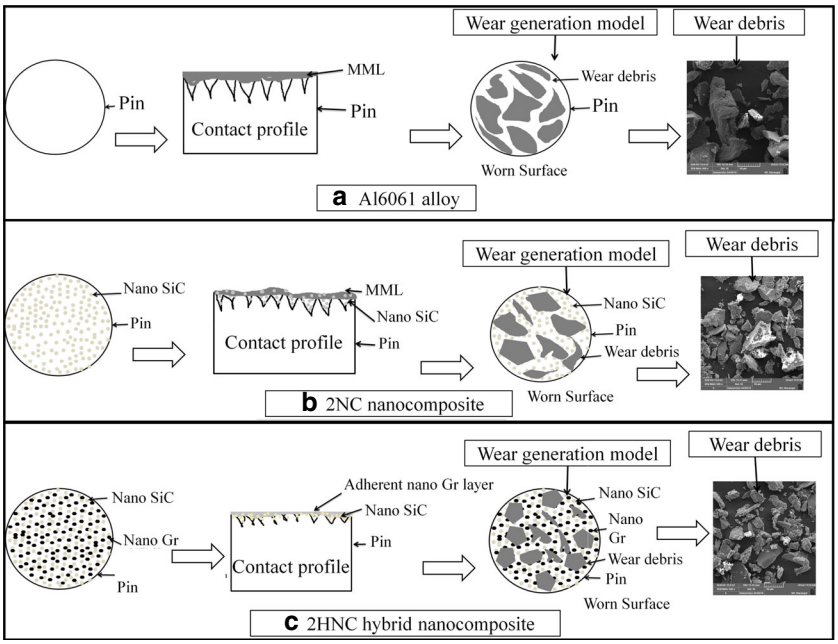

Fig. 15 Schematic view of wear generation model including wear debris of Al6061 alloy, 2NC nanocomposite and 2HNC hybrid nanocomposites

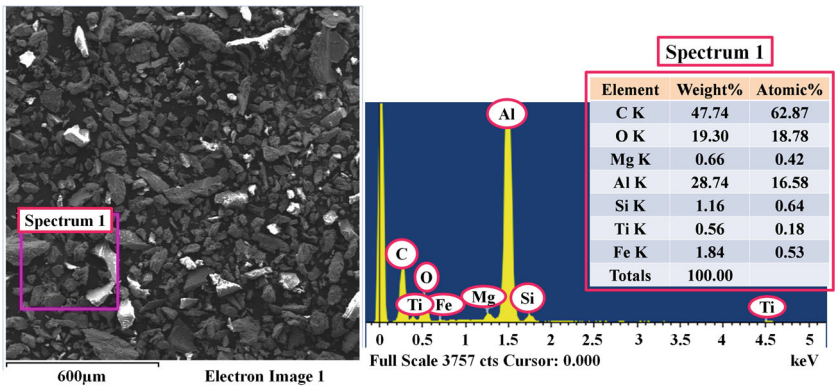

Fig. 16 EDAX analysis of wear debris of 2HNC hybrid nanocomposite

the EN31 steel disc to the worn surface of hybrid nanocomposite pin. Hard asperities at the interface of mating parts penetrate into the oxide layer and damage the oxide mixed layer. The presence of a high oxygen peak confirmed the oxidation process and the iron indicates the materials transition by adhesion at higher load 20 N.

4 Conclusions

The various nanocomposites such as 0.5HNC, 1HNC, 1.5HNC, 2HNC and 3HNC nanocomposites.are successfully produced through ultrasonically assisted casting technique. The following conclusions are drawn from the present study.

- SEM micrographs reveals uniform distribution of SiC and Gr nano-reinforcements in the Al6061 alloy matrix. However, small scale nano-clusters appeared in the microstructure with an increase of Gr.
- XRD pattern of hybrid nanocomposites exhibited the C and SiC peaks. The peaks are appeared when the content of Gr is higher quantity in the 2NC nanocomposite.
- Density of 0.5HNC, 1HNC, 1.5HNC, 2HNC and 3HNC hybrid nanocomposites is decreased by1%, 1.4%, 3.1%, 3.4%, and 4.3% respectively. The density of hybrid nanocomposites lowered due to the presence of lower density of Gr powder compared to the nanocomposite and base material.
- The average microhardness of Al6061 alloy, 2NC nanocomposite, 0.5HNC, 1HNC, 1.5HNC, 2HNC and 3HNC hybrid nanocomposites is observed to be (52 ± 3 HV), (91 ± 4 HV), (89 ± 2 HV), (87 ± 2 HV), (85 ± 2 HV), (83 ± 2 HV), and (76 ± 3 HV) respectively. Microhardness of hybrid nanocomposites increased compared to base alloy and decreased compared to nanocomposite. The reduction in microhardness of the hybrid nanocomposite could be due to presence of Gr.

- Reduction in wear rate of 2NC nanocomposite, 0.5HNC, 1HNC, 1.5HNC, 2HNC and 3HNC hybrid nanocomposites compared to Al6061 alloy at $L_HD_HV_H$ condition is 20%, 40.2%, 47.3%, 57%, 73%, and 64% respectively.
- Reduction in friction coefficient for 2NC nanocomposite, 0.5HNC, 1HNC, 1.5HNC, 2HNC and 3HNC hybrid nanocomposites compared to Al6061 alloy is 3%, 5.9%, 11.8%, 17.7%, and 9% respectively.
- The wear debris size decreased by reinforcing nano Gr in the 2NC nanocomposite.

4.1 Future Scope

The effect of cryogenic treatment on wear behaviour i.e., subsurface defromation, fretting wear, adhesive wear, two body and three body abrasive wear etc. can also be studied for Al-2SiC-Gr hybrid nanocomposites. Further, this study can be extended for various lubricating conditions with varied parameters.

References

1. Kaushik NC, Rao RN (2016) Effect of grit size on two body abrasive wear of Al 6082 hybrid composites produced by stir casting method. Tribol Int 102:52–60. https://doi.org/10.1016/j.triboint.2016.05.015
2. Prasad Reddy A, Vamsi Krishna P, Narasimha Rao R, Murthy NV (2017) Silicon carbide reinforced Aluminium metal matrix Nano composites-a review. Mater Today Proc 4:3959–3971. https://doi.org/10.1016/j.matpr.2017.02.296
3. Iredale R Manufacturing Composites for Automotive Applications. Univ Bristol 10–11
4. Soorya Prakash K, Balasundar P, Nagaraja S et al (2017) Effect of reinforcement, compact pressure and hard ceramic coating on aluminium rock dust composite performance. Int J Refract Met Hard Mater 54:223–229. https://doi.org/10.1108/ACMM-09-2017-1837
5. Reddy AP, Krishna PV, Rao RN (2017) Al/SiC $_{NP}$ and Al/SiC $_{NP}$ /X nanocomposites fabrication and properties: a review. Proc Inst Mech Eng Part N J Nanomater Nanoeng Nanosyst 231:155–172. https://doi.org/10.1177/2397791417744706
6. Soorya Prakash K, Gopal PM, Kavimani V (2017) Effect of rock dust, cenosphere and E-waste glass addition on mechanical, wear and machinability behaviour of Al 6061 hybrid composites. Indian J Eng Mater Sci 24:270–282
7. Al-Qutub AM, Khalil A, Saheb N, Hakeem AS (2013) Wear and friction behavior of Al6061 alloy reinforced with carbon nanotubes. Wear 297:752–761. https://doi.org/10.1016/j.wear.2012.10.006
8. Fallahdoost H, Nouri A, Azimi A (2016) Dual functions of TiC nanoparticles on tribological performance of Al/graphite composites. J Phys Chem Solids 93:137–144. https://doi.org/10.1016/j.jpcs.2016.02.020
9. Gupta P, Kumar D, Parkash O, Jha AK, Sadasivuni KK (2018) Dependence of wear behavior on sintering mechanism for Iron-alumina metal matrix nanocomposites. Mater Chem Phys 220:441–448. https://doi.org/10.1016/j.matchemphys.2018.08.079
10. Manivannan I, Ranganathan S, Gopalakannan S, Suresh S, Nagakarthigan K, Jubendradass R (2017) Tribological and surface behavior of silicon carbide reinforced aluminum matrix nanocomposite. Surfaces and Interfaces 8:127–136. https://doi.org/10.1016/j.surfin.2017.05.007
11. Mosleh-Shirazi S, Akhlaghi F, Yang LD (2016) Effect of SiC content on dry sliding wear, corrosion and corrosive wear of Al/SiC nanocomposites. Trans Nonferrous Met Soc China English Ed 26:1801–1808. https://doi.org/10.1016/S1003-6326(16)64294-2
12. Dehghan Hamedan A, Shahmiri M (2012) Production of A356-1wt% SiC nanocomposite by the modified stir casting method. Mater Sci Eng A 556:921–926. https://doi.org/10.1016/j.msea.2012.07.093
13. Saberi Y, Zebarjad SM, Akbari GH (2009) On the role of nano-size SiC on lattice strain and grain size of Al/SiC nanocomposite. J Alloys Compd 484:637–640. https://doi.org/10.1016/j.jallcom.2009.05.009
14. Kavimani V, Prakash KS, Gunashri R et al (2017) Tribological behaviour predictions of r-GO reinforced mg composite using ANN coupled Taguchi approach. J Appl Res Technol 110:430–441. https://doi.org/10.1108/ACMM-09-2017-1837
15. Stojanović B (2015) Application of aluminium hybrid composites in automotive industry. Teh Vjesn - Tech Gaz 22:247–251. https://doi.org/10.17559/TV-20130905094303
16. Mavhungu ST, Akinlabi ET, Onitiri MA, Varachia FM (2017) Aluminum matrix composites for industrial use: advances and trends. Procedia Manuf 7:178–182. https://doi.org/10.1016/j.promfg.2016.12.045
17. Dasgupta R (2012) Aluminium alloy-based metal matrix composites: a potential material for Wear resistant applications. ISRN Metall 2012:1–14. https://doi.org/10.5402/2012/594573
18. Prasad SV, Asthana R (2004) Aluminum metal-matrix composites for automotive applications: Tribological considerations. Tribol Lett 17:445–453. https://doi.org/10.1023/B:TRIL.0000044492.91991.f3
19. Koli DK, Agnihotri G, Purohit R (2015) Advanced Aluminium matrix composites: the critical need of automotive and aerospace engineering fields. Mater Today Proc 2:3032–3041. https://doi.org/10.1016/j.matpr.2015.07.290
20. Khodabakhshi F, Gerlich AP, Švec P (2017) Fabrication of a high strength ultra-fine grained Al-mg-SiC nanocomposite by multi-step friction-stir processing. Mater Sci Eng A 698:313–325. https://doi.org/10.1016/j.msea.2017.05.065
21. Şenel MC, Gürbüz M, Koç E (2018) Fabrication and characterization of synergistic Al-SiC-GNPs hybrid composites. Compos Part B Eng 154:1–9. https://doi.org/10.1016/j.compositesb.2018.07.035
22. Melaibari A, Fathy A, Mansouri M, Eltaher MA (2019) Experimental and numerical investigation on strengthening mechanisms of nanostructured Al-SiC composites. J Alloys Compd 774:1123–1132. https://doi.org/10.1016/j.jallcom.2018.10.007
23. Bajpai G, Purohit R, Rana RS, Singh Rajpurohit S, Rana A (2017) Investigation and testing of mechanical properties of Al-Nano SiC composites through cold isostatic compaction process. Mater Today Proc 4:2723–2732. https://doi.org/10.1016/j.matpr.2017.02.149
24. Hu K, Yuan D, Lü S Lin, Wu S Sen (2018) Effects of nano-SiCp content on microstructure and mechanical properties of SiCp/A356 composites assisted with ultrasonic treatment. Trans Nonferrous Met Soc China English Ed 28:2173–2180. https://doi.org/10.1016/S1003-6326(18)64862-9
25. Ravindran P, Manisekar K, Vinoth Kumar S, Rathika P (2013) Investigation of microstructure and mechanical properties of aluminum hybrid nano-composites with the additions of solid lubricant. Mater Des 51:448–456. https://doi.org/10.1016/j.matdes.2013.04.015

26. Kannan C, Ramanujam R (2018) Effectiveness evaluation of molten salt processing and ultrasonic cavitation techniques during the production of aluminium based hybrid nanocomposites - an experimental investigation. J Alloys Compd 751:183–193. https://doi.org/10.1016/j.jallcom.2018.04.112
27. Vishwanatha HM, Eravelly J, Kumar CS, Ghosh S (2017) Dispersion of ceramic nano-particles in the Al-cu alloy matrix using two-step ultrasonic casting and resultant strengthening. Mater Sci Eng A 708:222–229. https://doi.org/10.1016/j.msea.2017.09.117
28. Srivastava N, Chaudhari GP (2018) Microstructural evolution and mechanical behavior of ultrasonically synthesized Al6061-nano alumina composites. Mater Sci Eng A 724:199–207. https://doi.org/10.1016/j.msea.2018.03.092
29. Li J, Lü S, Wu S, Gao Q (2018) Effects of ultrasonic vibration on microstructure and mechanical properties of nano-sized SiC particles reinforced Al-5Cu composites. Ultrason Sonochem 42:814–822. https://doi.org/10.1016/j.ultsonch.2017.12.038
30. Xuan Y, Nastac L (2018) The role of ultrasonic cavitation in refining the microstructure of aluminum based nanocomposites during the solidification process. Ultrasonics 83:94–102. https://doi.org/10.1016/j.ultras.2017.06.023
31. Zhang D, Nastac L (2016) Numerical modeling of the dispersion of ceramic nanoparticles during ultrasonic processing of A356-based nanocomposites. Int J Cast Met Res 29:236–242. https://doi.org/10.1080/13640461.2016.1144266
32. Li Q, Qiu F, Dong BX et al (2018) Fabrication, microstructure refinement and strengthening mechanisms of nanosized SiC_P/Al composites assisted ultrasonic vibration. Mater Sci Eng A 735:310–317. https://doi.org/10.1016/j.msea.2018.08.060
33. Lan J, Yang Y, Li X (2004) Microstructure and microhardness of SiC nanoparticles reinforced magnesium composites fabricated by ultrasonic method. Mater Sci Eng A 386:284–290. https://doi.org/10.1016/j.msea.2004.07.024
34. Prasad Reddy A, Vamsi Krishna P, Rao RN (2020) Mechanical and Wear properties of aluminum-based nanocomposites fabricated through ultrasonic assisted stir casting. J Test Eval 48:20170560. https://doi.org/10.1520/JTE20170560
35. Srivastava N, Chaudhari GP (2016) Strengthening in Al alloy nano composites fabricated by ultrasound assisted solidification technique. Mater Sci Eng A 651:241–247. https://doi.org/10.1016/j.msea.2015.10.118
36. Ramesh KC, Sagar R (1999) Fabrication of metal matrix composite automotive parts. Int J Adv Manuf Technol 15:114–118. https://doi.org/10.1007/s001700050047
37. Zou XG, Miyahara H, Yamamoto K, Ogi K (2003) Sliding wear behaviour of Al-Si-cu composites reinforced with SiC particles. Mater Sci Technol 19:1519–1526. https://doi.org/10.1179/026708303225007997
38. Moazami-Goudarzi M, Akhlaghi F (2016) Wear behavior of Al 5252 alloy reinforced with micrometric and nanometric SiC particles. Tribol Int 102:28–37. https://doi.org/10.1016/j.triboint.2016.05.013
39. Mazahery A, Shabani MO (2013) Microstructural and abrasive wear properties of SiC reinforced aluminum-based composite produced by compocasting. Trans Nonferrous Met Soc China English Ed 23:1905–1914. https://doi.org/10.1016/S1003-6326(13)62676-X
40. Zeng X, Yu J, Fu D, Zhang H, Teng J (2018) Wear characteristics of hybrid aluminum-matrix composites reinforced with well-dispersed reduced graphene oxide nanosheets and silicon carbide particulates. Vacuum 155:364–375. https://doi.org/10.1016/j.vacuum.2018.06.033
41. Hekner B, Myalski J, Valle N, Botor-Probierz A, Sopicka-Lizer M, Wieczorek J (2017) Friction and wear behavior of Al-SiC(n) hybrid composites with carbon addition. Compos Part B Eng 108:291–300. https://doi.org/10.1016/j.compositesb.2016.09.103
42. Hariharasakthisudhan P, Jose S, Manisekar K (2018) Dry sliding wear behaviour of single and dual ceramic reinforcements premixed with Al powder in AA6061 matrix. J Mater Res Technol:1–9. https://doi.org/10.1016/j.jmrt.2018.01.005
43. Leng J, Wu G, Zhou Q et al (2008) Mechanical properties of SiC/gr/Al composites fabricated by squeeze casting technology. Scr Mater 59:619–622. https://doi.org/10.1016/j.scriptamat.2008.05.018
44. Carvalho O, Buciumeanu M, Madeira S, Soares D, Silva FS, Miranda G (2015) Dry sliding wear behaviour of AlSi-CNTs-SiCp hybrid composites. Tribol Int 90:148–156. https://doi.org/10.1016/j.triboint.2015.04.031
45. Aruri D, Adepu K, Adepu K, Bazavada K (2013) Wear and mechanical properties of 6061-T6 aluminum alloy surface hybrid composites [(SiC + gr) and (SiC + Al_2O_3)] fabricated by friction stir processing. J Mater Res Technol 2:362–369. https://doi.org/10.1016/j.jmrt.2013.10.004
46. Ravindran P, Manisekar K, Rathika P, Narayanasamy P (2013) Tribological properties of powder metallurgy - processed aluminium self lubricating hybrid composites with SiC additions. Mater Des 45:561–570. https://doi.org/10.1016/j.matdes.2012.09.015
47. Liu YB, Lim SC, Ray S, Rohatgi PK (1992) Friction and wear of aluminium-graphite composites: the smearing process of graphite during sliding. Wear 159:201–205. https://doi.org/10.1016/0043-1648(92)90303-P
48. W. Ames, A.T. Alpas (1995) Wear mechanisms in hybrid composites of graphite-20% SiC in A356 aluminium alloy (Al-7% Si-0.3% mg). Met mater trans a 26:85±98
49. Mostafapour Asl A, Khandani ST (2013) Role of hybrid ratio in microstructural, mechanical and sliding wear properties of the Al5083/$Graphite_p$/Al_2O_{3p} a surface hybrid nanocomposite fabricated via friction stir processing method. Mater Sci Eng A 559:549–557. https://doi.org/10.1016/j.msea.2012.08.140
50. Suresha S, Sridhara BK (2010) Effect of addition of graphite particulates on the wear behaviour in aluminium-silicon carbide-graphite composites. Mater Des 31:1804–1812. https://doi.org/10.1016/j.matdes.2009.11.015
51. Singh J (2016) Fabrication characteristics and tribological behavior of Al/SiC/gr hybrid aluminum matrix composites: a review. Friction 4:191–207. https://doi.org/10.1007/s40544-016-0116-8
52. Basavarajappa S, Chandramohan G, Mahadevan A, Thangavelu M, Subramanian R, Gopalakrishnan P (2007) Influence of sliding speed on the dry sliding wear behaviour and the subsurface deformation on hybrid metal matrix composite. Wear 262:1007–1012. https://doi.org/10.1016/j.wear.2006.10.016
53. Manivannan I, Ranganathan S, Gopalakannan S, Suresh S (2018) Mechanical properties and Tribological behavior of Al6061–SiC–gr self-lubricating hybrid nanocomposites. Trans Indian Inst Metals 71:1–15. https://doi.org/10.1007/s12666-018-1321-0
54. Saravanakumar A, Sasikumar P (2016) Dry sliding wear behaviour of Al6063/Al_2O_{3P}/Gr_P hybrid metal matrix composites. J Balk Tribol Assoc 22:1253–1264. https://doi.org/10.1108/00368791211262499
55. Reddy MP, Shakoor RA, Parande G, Manakari V, Ubaid F, Mohamed AMA, Gupta M (2017) Enhanced performance of nano-sized SiC reinforced Al metal matrix nanocomposites synthesized through microwave sintering and hot extrusion techniques. Prog Nat Sci Mater Int 27:606–614. https://doi.org/10.1016/j.pnsc.2017.08.015
56. Astm (2000) G 99: Standard Test Method for Wear Testing with a Pin-on-Disk Apparatus. Annu B ASTM Stand G-99-95a 1–5. https://doi.org/10.1520/G0099-05R10.2
57. Gupta R, Daniel BSS (2018) Impression creep behaviour of ultrasonically processed in-situ Al_3Ti reinforced aluminium composite. Mater Sci Eng A 733:257–266. https://doi.org/10.1016/j.msea.2018.07.017

58. Kumar N, Gautam G, Gautam RK, Mohan A, Mohan S (2016) Wear, friction and profilometer studies of insitu AA5052/ZrB_2composites. Tribol Int 97:313–326. https://doi.org/10.1016/j.triboint.2016.01.036
59. Omrani E, Moghadam AD, Menezes PL, Rohatgi PK (2016) Influences of graphite reinforcement on the tribological properties of self-lubricating aluminum matrix composites for green tribology, sustainability, and energy efficiency-a review. Int J Adv Manuf Technol 83:325–346. https://doi.org/10.1007/s00170-015-7528-x
60. Thirumalai Kumaran S, Uthayakumar M (2014) Investigation on the dry sliding friction and wear behavior of AA6351-SiC-B_4C hybrid metal matrix composites. Proc Inst Mech Eng Part J J Eng Tribol 228:332–338. https://doi.org/10.1177/1350650113508103
61. Menezes PL, Rohatgi PK, Lovell MR (2012) Self-lubricating behavior of graphite reinforced metal matrix composites. In: Nosonovsky M, Bhushan B (eds) Green tribology: biomimetics, energy conservation and sustainability. Springer Berlin Heidelberg, Berlin, Heidelberg, pp 445–480
62. Abdollahi A, Alizadeh A, Baharvandi HR (2014) Dry sliding tribological behavior and mechanical properties of Al2024-5wt.%B_4C nanocomposite produced by mechanical milling and hot extrusion. Mater Des 55:471–481. https://doi.org/10.1016/j.matdes.2013.09.024
63. Alizadeh A, Taheri-Nassaj E (2012) Mechanical properties and wear behavior of Al-2 wt.% cu alloy composites reinforced by B_4C nanoparticles and fabricated by mechanical milling and hot extrusion. Mater Charact 67:119–128. https://doi.org/10.1016/j.matchar.2012.02.006
64. Rajeev VR, Dwivedi DK, Jain SC (2010) Effect of load and reciprocating velocity on the transition from mild to severe wear behavior of Al-Si-SiCp composites in reciprocating conditions. Mater Des 31:4951–4959. https://doi.org/10.1016/j.matdes.2010.05.010
65. Rao RN, Das S, Mondal DP, Dixit G (2009) Dry sliding wear behaviour of cast high strength aluminium alloy (Al-Zn-mg) and hard particle composites. Wear 267:1688–1695. https://doi.org/10.1016/j.wear.2009.06.034
66. Baradeswaran A, Elaya Perumal A (2013) Influence of B_4C on the tribological and mechanical properties of Al 7075-B_4C composites. Compos Part B Eng 54:146–152. https://doi.org/10.1016/j.compositesb.2013.05.012
67. Kavimani V, Prakash KS (2018) Doping effect of SiC over graphene on dry sliding Wear behaviour of mg/SiC@r-GO MMCs and its surface characterization. Silicon 10:2829–2843. https://doi.org/10.1007/s12633-018-9823-2
68. Bastwros MMH, Esawi AMK, Wifi A (2013) Friction and wear behavior of Al-CNT composites. Wear 307:164–173. https://doi.org/10.1016/j.wear.2013.08.021
69. Akhlaghi F, Zare-Bidaki A (2009) Influence of graphite content on the dry sliding and oil impregnated sliding wear behavior of Al 2024-graphite composites produced by in situ powder metallurgy method. Wear 266:37–45. https://doi.org/10.1016/j.wear.2008.05.013
70. Wilson S, Alpas a TT (1997) Wear mechanism maps for metal matrix composites. Wear 212:41–49. https://doi.org/10.1016/S0043-1648(97)00142-7
71. Sameezadeh M, Emamy M, Farhangi H (2011) Effects of particulate reinforcement and heat treatment on the hardness and wear properties of AA 2024-$MoSi_2$ nanocomposites. Mater Des 32:2157–2164. https://doi.org/10.1016/j.matdes.2010.11.037
72. Mazahery A, Shabani MO (2012) Study on microstructure and abrasive wear behavior of sintered Al matrix composites. Ceram Int 38:4263–4269. https://doi.org/10.1016/j.ceramint.2012.02.008
73. Vencl A, Bobic I, Arostegui S, Bobic B, Marinković A, Babić M (2010) Structural, mechanical and tribological properties of A356 aluminium alloy reinforced with Al_2O_3, SiC and SiC+ graphite particles. J Alloys Compd 506:631–639. https://doi.org/10.1016/j.jallcom.2010.07.028
74. Rajkumar K, Aravindan S (2013) Tribological behavior of microwave processed copper–nanographite composites. Tribol Int 57:282–296. https://doi.org/10.1016/j.triboint.2012.06.023
75. Hosseini N, Karimzadeh F, Abbasi MH, Enayati MH (2012) A comparative study on the wear properties of coarse-grained Al6061 alloy and nanostructured Al6061-Al_2O_3composites. Tribol Int 54:58–67. https://doi.org/10.1016/j.triboint.2012.04.020